Article

An On-Line Sensor Fault Detection System for an AC Microgrid Secondary Control Based on a Sliding Mode Observer Model

John Bravo [1,*], Leony Ortiz [2,*], Edwin García [2], Milton Ruiz [2] and Alexander Aguila [2]

1   Faculty of Engineering in Mining, Petroleum and Environmental Geology, Universidad Central del Ecuador, Quito 170129, Ecuador
2   Electrical Engineering Department, Smart Grid Research Group—GIREI, Salesian Polytechnic University, Quito 170702, Ecuador; egarcia@ups.edu.ec (E.G.); mruizm@ups.edu.ec (M.R.); aaguila@ups.edu.ec (A.A.)
*   Correspondence: jgbravos@uce.edu.ec (J.B.); lortizm@ups.edu.ec (L.O.)

Abstract: The current study proposes a strategy for sensing fault detection in the secondary control of an isolated Microgrid based on a high-order Sliding Mode Robust Observers design. The proposed strategy's main objective is to support future diagnostic and fault tolerance systems in handling these extreme situations. The proposal is based on a generation system and a waste management system. Four test scenarios were generated in a typical Microgrid to validate the designed strategy, including two Battery Energy Storage Systems in parallel, linear, and non-linear loads. The scenarios included normal grid operation and three types of sensing faults (abrupt, incipient, and random) directly affecting the secondary control of a hierarchical control strategy. The results showed that the proposed strategy could provide a real-time decision for detection and reduce the occurrence of false alarms in this process. The effectiveness of the fault detection strategy was verified and tested by digital simulation in Matlab/Simulink R2023b.

Keywords: battery energy storage systems; distributed generation; microgrids; secondary control; sensing fault detection; sliding mode observers

1. Introduction

Climate policies aim to reduce greenhouse gas emissions from electricity consumption by encouraging both decarbonization of power supplies and optimal control of electric energy demand. Sustainable energy solutions, which have a minimal impact on climate change while potentially generating social, economic, and environmental benefits, are crucial and fundamental components for a successful transition to more sustainable energy systems. A shift towards distributed renewable electricity generation is considered a potential pathway to achieving various sustainability goals [1–3].

Microgrids (MGs) have emerged as a flexible architecture for implementing distributed renewable energy sources and various types of storage to meet the needs of different communities. Their operation, as required in both isolated mode and when connected to the main grid, applies to both urban districts and remote rural areas. If implemented appropriately, MGs can provide multiple technical, economic, social, and environmental benefits [4,5].

A Microgrid (MG) operating in isolated mode must consider the following main elements: Power Generation Sources, Battery Energy Storage Systems (BESSs), Control and Monitoring Systems, Load Controllers, and an Electrical Distribution Network. These aforementioned systems are not exempt from disturbances and electrical faults. If faults are not detected in a timely manner and corrective actions are not taken, MGs can lose stability and degrade their operation, which may even lead to a complete shutdown of Electrical Generation [6,7].

In this regard, addressing the problem of fault detection as a complement to the hierarchical control of Microgrids (MGs) is crucial for maintaining the reliability and

stability of MGs, even in the event of faults, as well as achieving a resilient integration of renewable energy sources. An effective fault detection mechanism with low processing effort that is capable of operating in real-time alongside hierarchical control would form part of the first phase to achieve fault tolerance and resilience in MGs.

This research aims to present methodologies and strategies for designing fault detection systems that enable rapid and precise identification of anomalies, thereby reducing downtime or preventing further damage due to the cascading effects of faults. Fault detection systems in MGs and Fault Tolerant Control (FTC) systems significantly impact energy efficiency by allowing a rapid and accurate response to anomalies and enabling their operation in such situations. This contributes to the reduction in losses and ensures continuous operation, even in extreme conditions.

Developing fault detection, identification, and management systems applied to Microgrids (MGs) has become a challenge for the scientific and academic community. Various fault detection methods can be employed in MGs, including model-based methods such as state estimators, classification-based methods, and domain transformation methods, among others [2,8,9].

As mentioned, the authors in ref. [10] proposed an innovative method for Control Reconfiguration based on Model Predictive Control (MPC). The research encompassed fault detection, isolation, and the subsequent reconfiguration of the system. The method is based on the use of parity equations, structured residuals, and stochastic thresholds to identify system faults. On the other hand, reconfiguration is achieved by adapting the control law to the new conditions created by the presence of a fault phenomenon.

In ref. [11], a Fault-Tolerant Distributed Secondary Controller is proposed to address the issue of unknown False Data Injection Attacks (FDIA) in a DC MG. An exhaustive analysis of the impact of FDIA signals on the MG is conducted, and a Distributed Extended State Observer (DESO) is developed to detect these signals by calculating the relative output error between distributed generators and their neighbors. Subsequently, a fault-tolerant secondary controller is designed to counteract the adverse effects of attack signals on the system, using the FDIA signals detected by the DESO observer as a basis.

Another approach is proposed in ref. [12], where the authors introduce a multi-resolution analysis using a discrete wavelet transform to detect traveling wave components across different frequency ranges in direct current (DC) fault currents. Subsequently, the method calculates the Parseval energy of the coefficients from the multi-resolution analysis. This demonstrates a quantitative relationship between the fault current signal's energy and the coefficients' energy. The calculated Parseval energy values are used to train a Support Vector Machine (SVM) classifier to identify the type of fault effectively.

On the other hand, in ref. [13] a fault detection method for DC MGs is proposed based on the principle of a residual generating function. By evaluating the residual error of each line and designing a detection threshold, the method achieves fault detection for multiple converters connected to an MG. Conversely, the authors in ref. [14] designed an overlaid phase current scheme with a voltage restraint element that accurately identifies both symmetrical and asymmetrical short-circuit faults within half a cycle (<10 ms). The proposed scheme can be included in both conventional and communication-assisted classification schemes for protection coordination purposes.

The FTC method proposed in ref. [15] is based on the recursive online estimation of a reduced-order model and the generation of a residue using the Kalman filter. Subsequently, they employed a two-sided cumulative sum (CUSUM) sequential change detection algorithm to identify faults in sensors or communication links.

In ref. [16], an algorithm for detecting and classifying faults in a power transmission line is presented. This work's key contribution is calculating the correlation coefficient between the current signal of each phase in the three-phase system and its reference value. The proposed algorithm is characterized by its simplicity and practicality, as it solely relies on measuring the current at the local terminal.

At the same time, the sensor fault detection approach proposed in ref. [17] relies on the online estimation of the recursive model and an observer based on residual generation. Using an estimated model and Kalman linear filters, residual signals are generated which are used by a sequential change detection unit to determine whether the system is in normal operating mode or if a fault has occurred.

In ref. [18], a scheme for detecting and compensating smart sensor faults in a hybrid network is described. The sensors involved in the control algorithm may not be ideal, and, if a fault occurs, the system could collapse. Another study primarily focuses on developing a scientific methodology for the design of Fault-Tolerant Centralized Hierarchical Control Systems for Sensors within the context of isolated Microgrids (MGs). The methodology developed by the authors is based on a modified Kalman filter algorithm. It also proposes a novel fault detection methodology using a reconfigurable estimator. Additionally, this method is computationally efficient, fast, and easy to implement and adjust, making it feasible for more complex control configurations, multiple sensor faults, and different hierarchical levels of control [8].

The scientific article proposed in ref. [19] presents a sliding mode control scheme based on observers to suppress flexion–torsion (flutter) coupling vibrations in an aeroelastic wing system with delayed output using piezoelectric actuators. The flutter speed and frequency of the closed-loop system with delay are obtained by solving a polynomial eigenvalue problem. In this context, the authors develop a state observability-based controller, independent of time delay, with gain matrices obtained through Linear Matrix Inequalities (LMIs), aiming to ensure the asymptotic stability of the system. The simulation results shown in this article demonstrate that the control strategy is effective in suppressing flutter in systems with delayed output. Indeed, the impact of time delay is significant on the flutter speed and frequency; however, its aeroelastic response can be stabilized in a finite time with the implementation of this type of observer-based SMO controller. Continuing with our systematic literature review, we find other contributions, such as predictive control methods, which are characterized by their simplicity and robustness [20]. In this case, the voltage sensor used for rectifier feedback is lost. The proposed control recalculates the AC input voltage to estimate instantaneous powers (active and reactive) using alternative variables such as input currents, the voltage of the link, and the switching state.

As observed in the previous literature, there are various challenges in implementing and operating MGs, mainly in isolated mode, due to the nature of renewable energy sources, BESSs, the continuous operation regime of MGs, and the underlying metrological conditions. The transition towards a sustainable energy matrix covers one of the most significant scientific challenges, which is research into the detection of sensing failures (internal or external to the control system). In MGs, research responds to the critical need to ensure the operational stability and reliability of these systems, as it plays a crucial role in making timely decisions for fault tolerance and alleviating the problem. This prevents a sudden energy inconvenience due to successive failures of key MG components.

The consulted literature review reveals several significant gaps. In particular, there is a need to develop studies with systems that are more efficient yet simpler in design and adjustment, with low processing effort, and with acceptable real-time performance. Although a variety of existing studies use sophisticated data-based or model-based methodologies, the impact of a simpler and more robust strategy like the one proposed in this research directly affects practical scenarios with multiple simultaneous faults. Additionally, it could constitute a crucial link for the integration of these systems with emerging communication and cybersecurity technologies.

This research seeks to optimize the use of energy resources, address specific technological challenges, and strengthen resilience against external threats (such as possible cyberattacks) for the sake of a safer, more efficient, and sustainable energy transition. The feedback sensing fault detection strategy proposed for parallel-connected BESSs will contribute to developing new fault tolerance systems applied to hierarchical control systems, thereby improving the reliability and resilience of MGs and their power elements. To

achieve this, a fault detection algorithm based on parameter estimation and residue generation using Robust Sliding Mode Observers (SMOs) will be designed, and the residue will be managed using statistical strategies, thus promoting the continuous improvement of these fundamental systems.

2. Materials and Methods

Sensing failures or measurement system errors can arise from various causes, both non-malicious phenomena (such as the wear and tear of the components that make up the measurement chain) and malicious phenomena (such as cyber-attacks). In most cases, sensing failures lead to the partial or abrupt deterioration of the control law, often resulting in the loss of observability and controllability of the MG [8,21–24]. The study of algorithms for fault diagnosis is part of an initial phase in FTC methodologies, as well as error mitigation and management systems [25].

This study implements the modeling and simulation of the MG under study using Matlab®/Simulink R2023b. This implementation includes methodologies such as the dynamic identification of the plant and the different systems and subsystems of the MG. To validate the proposal, various types and events of sensing failures associated with the feedback loop of the secondary control of the hierarchical system were simulated.

2.1. Robust Estimation of Sensing Failures

In recent years, SMO-based sensor fault estimation methods have been widely studied due to their inherent robustness in modeling uncertainties and disturbances. Based on [26], a sensor failure estimation scheme for uncertain Lipschitz non-linear systems is presented below which includes the effects of system uncertainties and is used to eliminate the effects of system uncertainties.

The following SMO is used to estimate sensing failures:

$$
\begin{cases}
\dot{\hat{Z}}_1 = A_1\hat{Z}_1 + \overline{A}_2\hat{Z}_0 + W_1 f\left(T^{-1}\hat{Z}, t\right) + B_1 u + \frac{1}{2}\hat{k}_1 P_1 C_1^{-1}(w_1 - \hat{w}_1) + \ldots \\
\qquad \ldots + (A_1 - A^s{}_1)C^{-1}{}_1(w_1 - \hat{w}_1) + v_1 \\
\qquad\qquad \hat{w}_1 = C_1\hat{Z}_1
\end{cases}
\tag{1}
$$

where:

- $f(x, t) \in \mathcal{R}^j$ is the non-linear term;
- $A \in \mathcal{R}^{nxn}, B \in \mathcal{R}^{nxn}$ are constant state space matrices;
- $A^s{}_1 \in \mathcal{R}^{rxr}$ is a stable matrix that needs to be determined;
- P_1 is the Lyapunov matrix of $A^s{}_1$, $\hat{Z} := \left[\left(C_1^{-1}S_1 y\right)^T, \ \left([I_{n-r}\ 0]\hat{Z}_0)^T\right.\right]^T$;
- v_1 is the discontinuous output error;
- $w_1 \in \mathcal{R}^r, \ A_1 \in \mathcal{R}^{rxr} y \ W_1 \in \mathcal{R}^{rxj}$ are coordinated by the system;
- $\overline{A}_2 = \left[A_2 \ 0_{rx(p-r)}\right]$.

State estimation error dynamics after the occurrence of sensor failures.

If state estimation errors are defined by $e_1 = z1 - \hat{z}1$ and $e_0 = z0 - \hat{z}0$, then the dynamic estimation of the error after the occurrence of the fault can be obtained from:

$$
\dot{e}_1 = A^s{}_1 + \overline{A}_2 e_0 + W_1(f(T^{-1}z, t) - f(T^{-1}\hat{z}, t)) - \frac{1}{2}\hat{k}_1 P_1 e_1 + E_1\Delta\Psi - v_1
\tag{2}
$$

$$
\dot{e}_0 = (A_0 - L_0 C_0)e_0 + \overline{W}_2(f(T^{-1}z, t) - f(T^{-1}\hat{z}, t)) - \frac{1}{2}\hat{k}_2 \overline{W}_2 H_0 C_0 e_0
\tag{3}
$$

The time derivative of V can be obtained by:

$$\dot{V} = \dot{V}_1 + \dot{V}_2 + \dot{V}_3 + \dot{V}_4 \leq e_1^T \Pi_1 e_1 + 2e_1^T P_1 \overline{A}_2 e_0 + e_0^T \Pi_2 e_0 + 2\|e_0\|^2$$
$$= \begin{bmatrix} e_1 \\ e_0 \end{bmatrix}^T \begin{bmatrix} \Pi_1 & P_1\overline{A}_2 \\ \overline{A}_2^T P_1 \Pi_2 & + 2I_{n+p-2r} \end{bmatrix} \begin{bmatrix} e_1 \\ e_0 \end{bmatrix} \tag{4}$$

Since $\dot{V} < 0$, this implies that the observer error dynamics are asymptotically stable.

With respect to the Lipschitz constant, it is often difficult to know precisely its value, but the asymptotic estimation of the states can be guaranteed even if the estimates of $k_1 y k_2$ are not close to their real values.

The state estimation errors are asymptotically stable, so, for the dynamics of the errors, the sliding mode surface is defined by the following:

$$\ell = \{(e_1, e_0)|e_1 = 0, C_0 e_0 = 0\} \tag{5}$$

where:

- δ is the positive scalar useful to reduce the vibration effect.

2.2. Proposed Fault Detection Strategy

In this section, the proposed strategy for the design of the sensing fault detection system is presented. This strategy is designed using an optimal estimation system based on the system model. For this purpose, a Sliding Mode Observer (SMO) is implemented with the aim of establishing a residue generation system from the difference between the estimated value of the variable and its sensed value at the input of the Control System (CS).

The SMO is initially designed based on the state space (SS) model of the Battery Energy Storage System (BESS). The SS is obtained from the secondary level of control in normal operating mode or in the absence of faults. The chosen SMO presents a high order due to the system model, precision, and stability, parameters required for the timely and accurate detection of sensing faults in real-time.

Figure 1 shows the Fault Detection System (FDS), which uses the observed or sensed signals of voltage, current, and positive sequence reactive power from the calibration model to estimate the states required for detection. When the obtained residue has a value close to zero, it indicates that there are no faults. However, this criterion is not sufficient for timely detection; therefore, it is necessary to complement the residue generation system with another system capable of handling and evaluating it. The proposed residue evaluation method is based on the mean value algorithm that seeks to achieve better statistical separability of the residue among different classes. This way, false positives resulting from comparing upper and lower thresholds are reduced. A false positive represents imprecise data that occur when the detection system incorrectly obtains a failure indicator residue when it is not actually present.
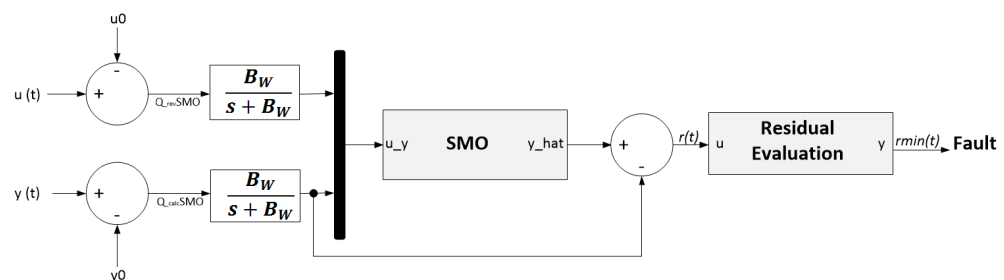

Figure 1. Sensing fault detection system.

Table 1 displays the variables used in the fault detection system's design. Algorithm 1 presents the main algorithm proposed for the fault detection strategy based on the SMO. For this, the estimated or observed residue $r(t)$ uses the inputs ($u(t)$ and $y(t)$) from the

CS for the BESSs. Following this, a boolean fault flag ("0" or "1") is raised to indicate the presence of one of the sensing fault classes.

Table 1. Detection system variables.

Symbology	Characteristic
u (*t*)	Input of the secondary control system.
y (*t*)	Output of the secondary control system or control action.
A, *B*, *C*, *D*	Matrices of the system model in SS (State Space).
Bw	Bandwidth of the sensing filter.
uo_V_ref; *yo_Q_calc1*; *yo_IaSC*; *yo_Va11*; *Ia11*	Initial conditions of the selected operating point.
Gn	Sliding Mode Observer gain matrix to set the observer dynamic.
P	Sliding Mode Observer weight matrix to set the Lyapunov function and ensure its stability.
L	Sliding Mode Observer gain matrix to correct the estimation error.
r (*t*)	Residue generated by the difference between the estimated and the sensed Q+ value.
Meanh	Mean value of the residue for the normal operation class.
Meanf	Mean value of the residue for the fault operation classes.
Fault_flag	Fault flag.
sys_ctrb	Controllability of the system.
sys_obs	Observability of the system
umbral+, *umbral−*	Thresholds +/−

Algorithm 2 shows the SMO design function, which calculates the observer's values of *Gn*, *P*, and *L* to obtain the signal *r* (*t*). Key inputs in the design of the SMO include the dynamic system's *A*, *B*, *C*, and *D* matrices in SS. It is important to emphasize that the method must verify the controllability of the SS (*sys_ctrb*) and its observability (*sys_obs*) to perform an additional check of the previously obtained SS model.

Algorithm 1: Main algorithm.

Step 1: **Inputs**: [*u*(*t*), *y*(*t*)];
Step 2: **Outputs**: {r (*t*), *Fault_flag* (0, 1), *observador_SMO* (*Gn*, *P*, *L*)};
Step 3: **Initialize:** *uo_V_ref* = 1; *uo_w_ref1* = 377; *yo_Q_calc1* = 47083;
　　　　　yo_IaSC = 413.553; *yo_Va11* = 1.0057; *yo_Ia11* = 521.821;
　　　　　Bw = 65; *uo* = [*uo_V_ref*, 3, *uo_w_ref1*];
　　　　　yo = [*yo_Q_calc1*, *yo_IaSC*, *yo_Va11*, *yo_Ia11*]; [*A*, *B*, *C*, *D*] = [ ];
Step 4: [*A*, *B*, *C*, *D*] ← *ident_función* (*u*, *y*);
Step 5: [*G$_n$*, *P*, *L*] ← *SMO_función* [*A*, *B*, *C*, *D*]; *observer_SMO* (*G$_n$*, *P*, *L*);
Step 6: [*r*, *y*, *ŷ*] ← *sim* (*Simulink_model*);
Step 7: *Fault_flag* ← *eval_resid* (*r*, *y*, *ŷ*);
Step 8: **Return** {*r*, *Fault_flag*, *observer_SMO*};

Algorithm 2: Robust Sliding Mode Observer function.

Step 1: **Inputs**: [*A*, *B*, *C*, *D*];
Step 2: **Outputs**: {*G$_n$*, *P*, *L*};
Step 3: **Initialize:** lambda$_1$ = −10; *lambda$_2$* = −15; *lambda$_3$* = −20; *lambda$_4$* = −25; *P* = [0.1];
Step 4: *sys_ctrb* ← *ctrb* (*A*, *B*); *rank* (*sys_ctrb*);
　　　　　sys_obs ← *obsv* (*A*, *C*);
　　　　　n ← *size* (*A*, 1); *m* = *size* (*B*, 2); *p* = *size* (*C*, 1)
　　　　　N$_c$ ← *null* (*C*); *A$_c$* ← *N$_c$* (1:*n*, 1:(*n*:*p*)); *T$_c$* ← [*N$_c$^{T}*; *C*];
　　　　　B$_c$ ← *T$_c$* × B; *C$_c$* ← C × (*T$_c$$^{-1}$*);
　　　　　L ← *place* (*A^T*, *C^T*, [*lambda$_1$*, *lambda$_2$*, *lambda$_3$*, *lambda$_4$*])^T;
　　　　　[*G$_n$*] ← *inv* (*T$_c$*) × [*L*, *-eye(p)*];
Step 8: **Return:** {*G$_n$*, *P*, *L*};

The algorithm presented in Algorithm 3 is implemented to evaluate the residues coming from the generation system, thus enabling the decision-making process for fault

detection in the sensing system. Initially, input variables are defined as a data vector $[r, y, \hat{y}]$. Subsequently, the data vector length and the analysis window are initialized.

Algorithm 3: Residue evaluation function.

Step 1: **Inputs**: $[r, y, \hat{y}]$;
Step 2: **Outputs**: {*Fault_flag*};
Step 3: **Initialize** $N = length\ (r)$; $vent = 1$;
Step 4: **if** $vent == 0$;
      $vent = 100$; $meanh \leftarrow zeros\ (N - vent + 1, 1)$;
      $meanf \leftarrow zeros\ (N - vent + 1, 1)$;
      for $i == 1$ **to** $N - vent + 1$;
          $meanh\ (i) \leftarrow \frac{\sum_{j=1}^{N} r(i:vent+i-1)}{N}$; $meanf\ (i) \leftarrow \frac{\sum_{j=1}^{N} r(i:vent+i-1)}{N}$; **end for**;
    else
      $vent = 100$; $meanh \leftarrow zeros\ (N - vent + 1, 1)$; $meanf \leftarrow zeros\ (N - vent + 1, 1)$;
      for $i = 1$ **to** $N - vent + 1$;
          $meanh\ (i) \leftarrow \frac{\sum_{j=1}^{N} r(i:vent+i-1)}{N}$; $meanf\ (i) \leftarrow \frac{\sum_{j=1}^{N} r(i:vent+i-1)}{N}$; **end for**; **end if**;
Step 5: $Thresholds + \leftarrow 1.1 \times max\ (meanf)$; $Thresholds - \leftarrow 1.1 \times min\ (meanf)$;
Step 6: **If** $meanf > Thresholds +$ **y** $meanf < Thresholds -$;
      $Fault\_flag = 1$;
    else
      $Fault\_flag = 0$; **end if**;
Step 7: **Return:** {Fault_flag};

---

3. Case Study

The MG depicted in Figure 2 is intricately designed and based on a calibration model. This MG is capable of operating in both isolated mode and connected to a main grid. The switching between operational modes is facilitated by a disconnector at the Point of Common Coupling (PCC). For the validation of the current proposal, the FDS is implemented in the MG described in Figure 2, operating in isolated mode. The validations were conducted in a digital simulation environment using Matlab/Simulink/Simscape R2023b based on the model described in [23] and using a sampling period of 0.002 s. The computer used in this study (simulations, algorithm design, and result analysis) is equipped with an Intel® Xeon® E-2276M processor, which operates at a frequency of 2.80 GHz. This processor is supported by 64.0 GB of EEC RAM, of which 7 GB are usable, which ensures a high data handling capacity and processing stability. Additionally, the system features an NVIDIA Quadro T2000 graphics card, which provides superior graphics performance and is ideal for scientific and engineering applications.
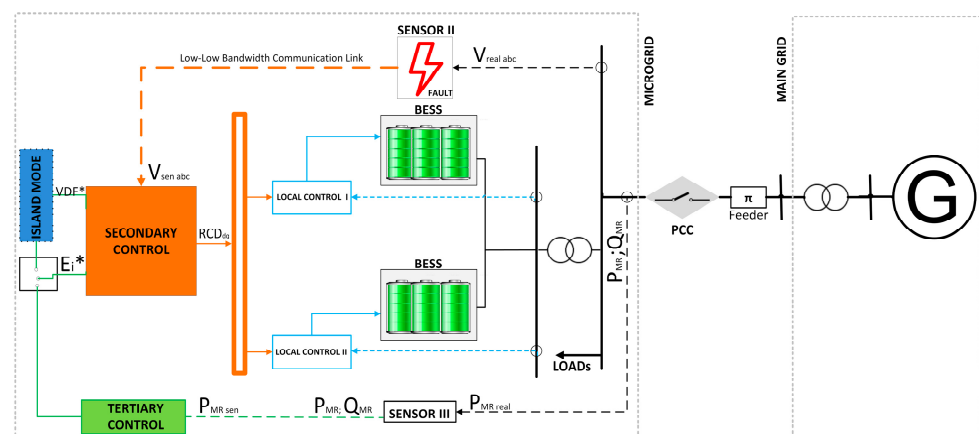

Figure 2. Single-line diagram case study.

The MG operates at 60 Hz and includes two parallel BESS storage sources in linear and non-linear loads. The BESSs are connected in parallel, operating on the AC bus. Each BESS consists of three nickel-metal hydride (Ni-MH) batteries at a nominal voltage of 650 VDC. The batteries connected in parallel are linked to a controlled inverter that boosts the voltage from 650 VDC to 900 VAC [23]. Both BESSs are connected via a bidirectional boost-buck converter interconnected through a cascaded topology.

In this research, the strategy is proposed to be validated by exposing it to classes of faults such as abrupt, random, and incipient faults at the time instant of 1 s. The aim is to establish the criteria for dynamic behavior in the face of faults that are severe and more likely to occur. All generated fault classes are in the sensing system corresponding to the feedback of the secondary control, as shown in Figure 2.

As demonstrated by the results, the dynamic behavior of the strategy during normal operation exhibits a stable performance that is capable of distinguishing between normal disturbances and actual faults. In the case of abrupt faults, the observer stabilizes and the faulty residues exhibit a greater amplitude, facilitating their detection.

Based on the analysis of the obtained results, it is shown that the sensing fault detection strategy for the CS using SMO for isolated AC MGs is feasible for application in this type of problem. Overall, the proposed strategy, combined with a fault tolerance system, will contribute to improving the reliability and safety of secondary control systems and MGs, providing a solid foundation for its implementation in similar cases.

3.1. Case Study No.1: Normal Operating Class

Figure 3 shows the dynamic behavior of variables such as current and AC bus voltage under normal operating conditions (without fault conditions). As can be seen, the *rms* value for both voltage and current demonstrates proper system operation, even in the presence of an unbalanced system. One second into operation, an abrupt load disturbance occurs, causing a typical minor variation in voltage that is immediately compensated for by the MG's hierarchical control and the BESS. The load disturbance results in a reduction in the active and reactive power of the MG's electrical system (Figure 4).

On the other hand, Figure 5 displays the residue variable generated by the residue generation system $r(t)$. As observed, the SMO stabilizes immediately both at system startup and in response to the load disturbance, consistently following the same trend. Under these conditions, the residue generation system operates normally, based on an accurate estimation by the SMO. Figure 5 shows that, while the generated residue $r(t)$ under operating conditions without sensing faults tends to zero, it is not feasible to directly establish detection thresholds. The challenge in performing direct detection based on the residue is due to the fact that a load disturbance also deteriorates it, leading to potential false positives in the future. Therefore, the failure thresholds are defined as follows: the upper threshold value is set to 5% above the maximum value of the residual function corresponding to the normal operation class. On the other hand, the value of the lower threshold is set at 5% below the minimum value of the residual function of the same class of normal operation. Figure 6 shows the response of the residue management system. It illustrates how the mean value of the residue $r_m(t)$ free from faults remains within the normal operation thresholds established by the algorithm, allowing for the differentiation of the dynamic effect of a load disturbance from an actual fault, as illustrated in Figure 7.
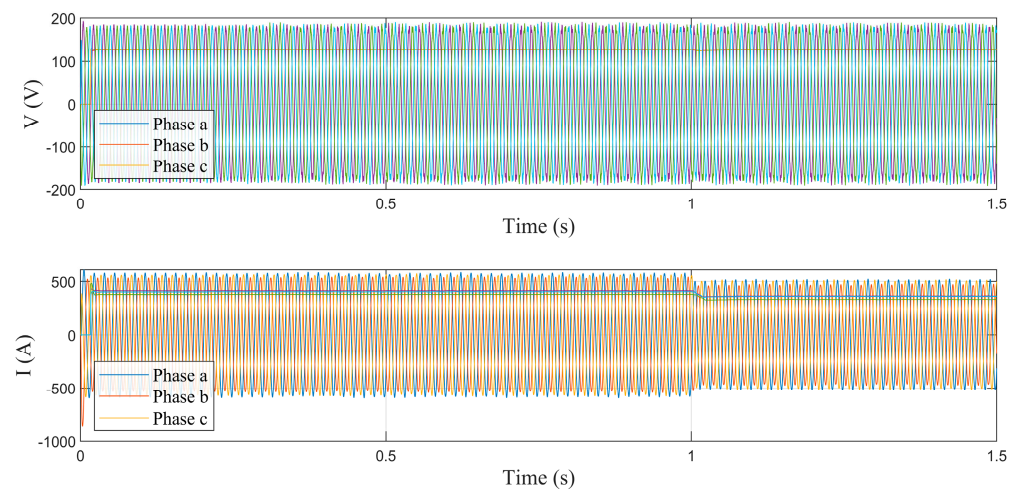
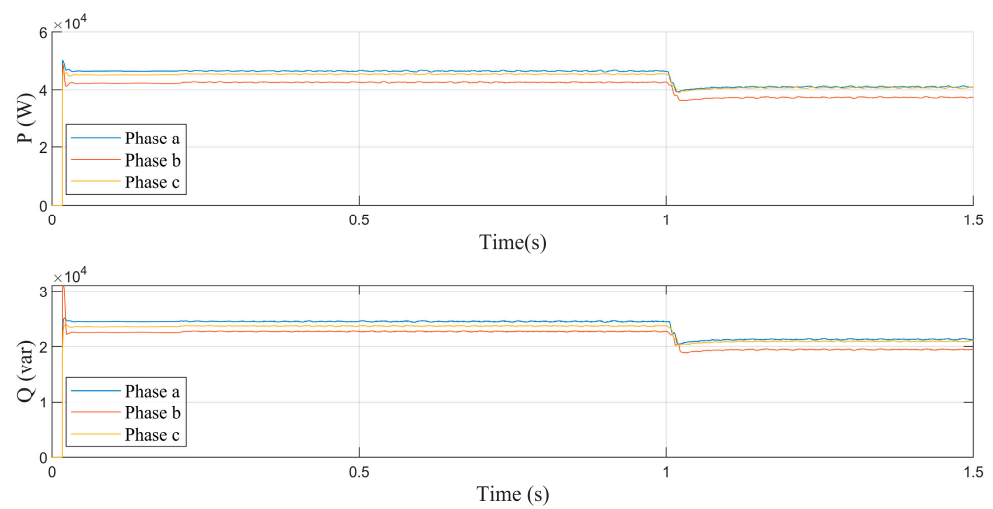**Figure 3.** Microgrid voltage and current; normal operation.

Figure 4. Active and reactive power in the Microgrid; normal operation.
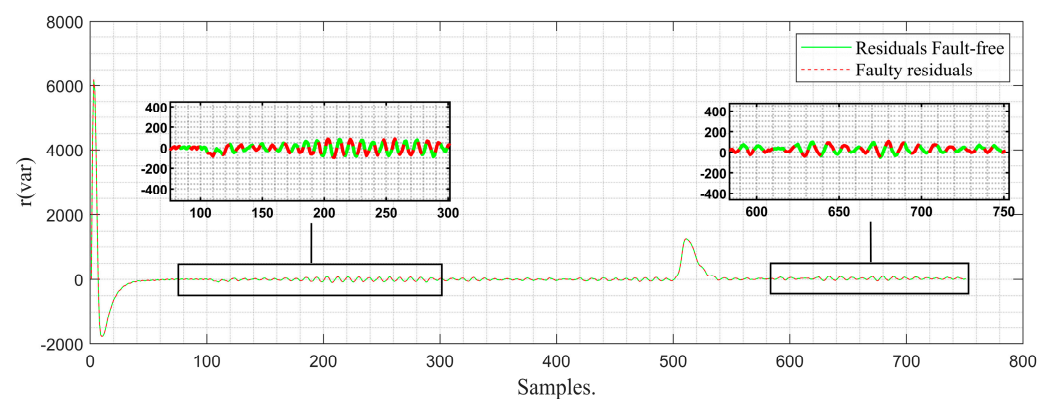

Figure 5. Waste generation system; normal operation.
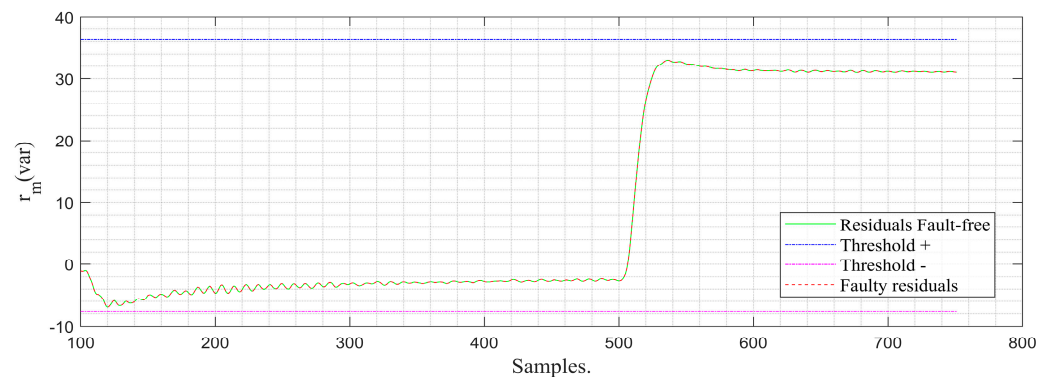
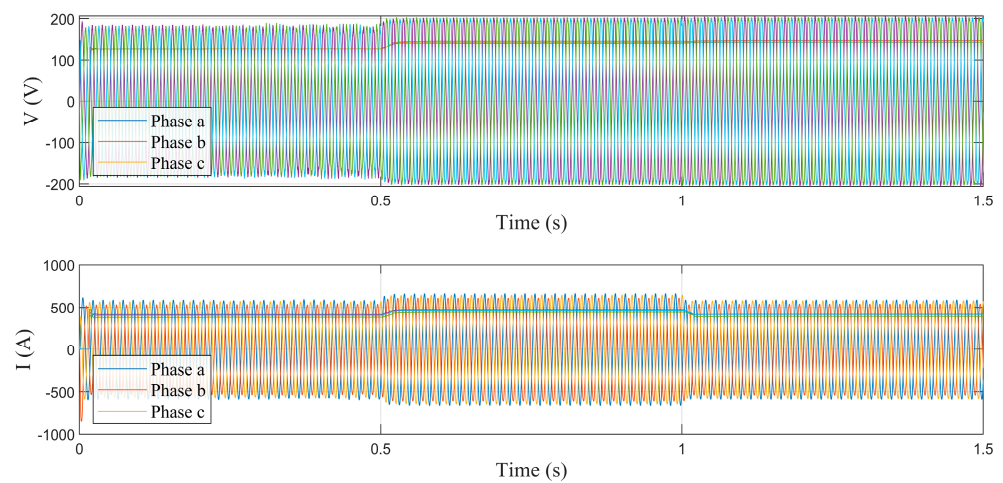**Figure 6.** Waste handling and failure detection system: mean value of $r(t)$; normal operation.

Figure 7. Microgrid voltage and current; abrupt failure.

3.2. Case Study No.2: Abrupt Failure Class

Figures 7 and 8 depict the dynamic behavior of voltage, current, active, and reactive power variables, similar to Figures 3 and 4, but this time in the presence of an abrupt sensing fault. In this case, a significant change is observed at the moment of fault occurrence (0.5 s). Similar to the previous case, the dynamic effect generated by the fault is very similar to that caused by the load disturbance at 1 s. This is largely due to the incorrect decision made by the control system due to the effect of the fault on its feedback loop. At this point, it is not an irregular behavior of the system, as the sudden increase in voltage causes a deterioration greater than 10% of it.

The abrupt fault induced in the sensing system at 0.5 s is then processed by the proposed FDS (Figure 10). Initially, Figure 9 shows the signal of the fault-free residue (t < 0.5 s) and the faulty residue (t ≥ 0.5 s) obtained at the output of the residue generation stage. Once the SMO stabilizes, a difference between the fault-free residues and the faulty residues is observed, resulting in a residue that is of greater amplitude but that is insufficient in regard to differentiating its effect compared to the load disturbance. Detecting the fault using the residue $r(t)$ alone is not sufficient, as other common system disturbances generate false alarms. Therefore, the residue management system achieves separability (Figure 10) between the two classes, enabling fault detection and reducing the likelihood of false alarms due to disturbances in normal operation.
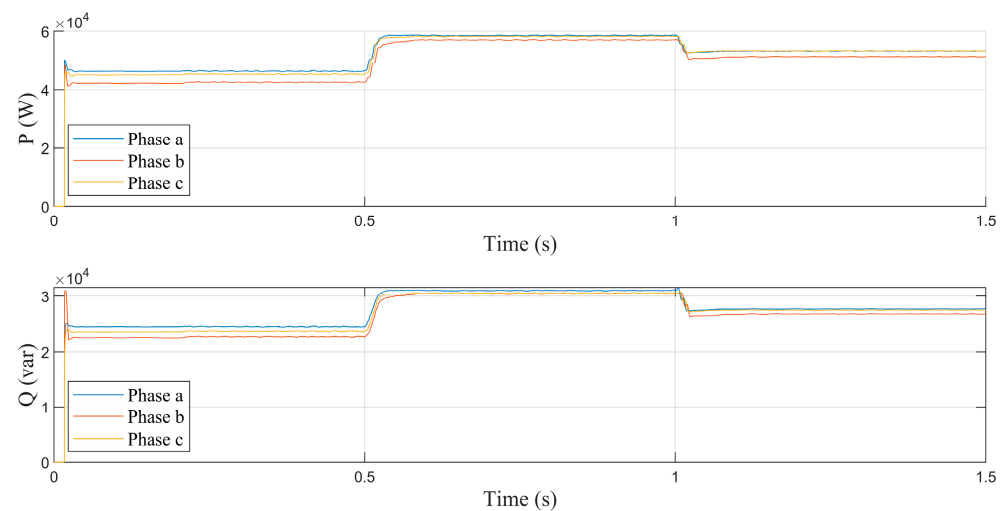
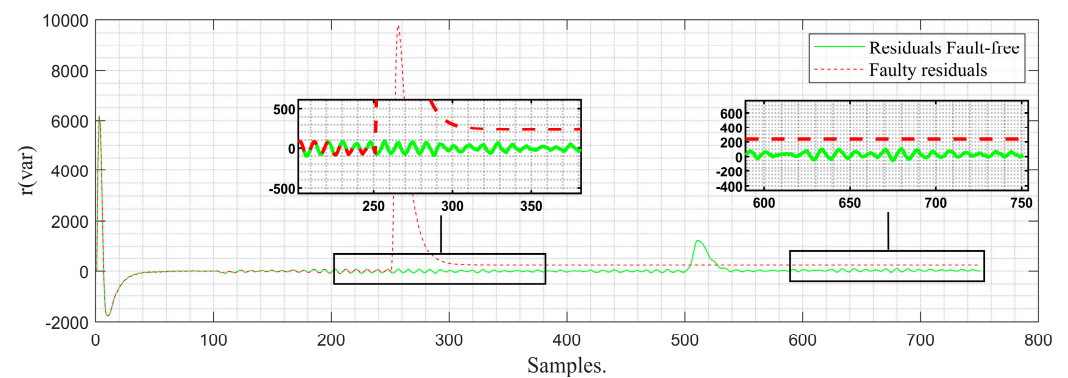**Figure 8.** Active and reactive power in the Microgrid; abrupt failure.

Figure 9. Residue generation system; abrupt failure.
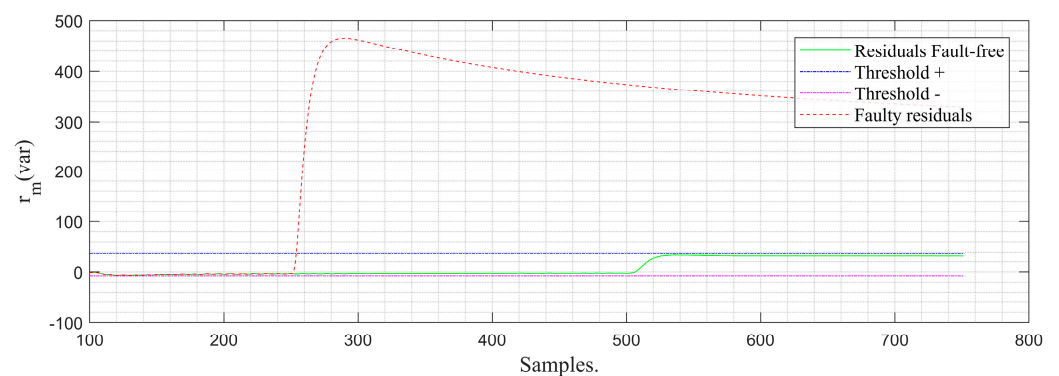

Figure 10. Residual handling system and failure detection: mean value of $r(t)$; abrupt failure.

In Figures 10 and 11, the response of the proposed system for residue evaluation is observed. By generating greater separability of the faulty residue, the mean residue $r_m(t)$ allows for the establishment of appropriate thresholds to ensure detection. Detection relies on the constant monitoring of $r_m(t)$ to determine whether $r_m(t)$ remains within the $+/-$ threshold limits. The moment $r_m(t)$ falls outside the tolerance band defined by the thresholds, a fault flag is raised (from 0 to 1), indicating the occurrence of a sensor fault. In a real (physical) system, it would be recommended to replace the sensor to allow the system to return to normal operation.
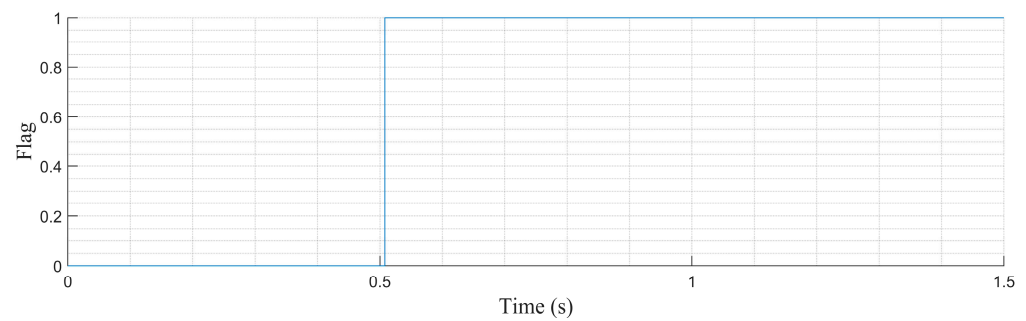
Figure 11. Failure flag; abrupt failure.

3.3. Case Study No.3: Incipient Failure Class

In this section, the proposed FDS is studied in the context of an incipient fault caused by the deterioration or degradation of the sensing system of the secondary control. Similar to other fault scenarios, the effect of the incipient fault in the sensor leads to inefficient operation of the secondary control action. As a result, the voltage profile either gradually decreases or increases depending on the slope of the type of incipient fault. In this case, the residue generation system exhibited behavior very similar to normal operation, which may indicate difficulty in the immediate detection of incipient sensor faults by the MG protection system.

In Figure 12, the behavior of the incipient (progressive) failure can be seen. As time goes by, it can be observed that the observer's signal and that of the fault-free residues do not present a visible difference, which is why, in this instance, it is not possible to determine the existence of a fault by delineating a tolerance band. For this reason, it is necessary to apply the residue management algorithm, thereby achieving greater separability between faulty residues and fault-free residues, as shown in Figure 13. As a result, the occurrence of the sensing fault based on the faulty residue can be determined due to the existing difference between the faulty residue and the fault-free or normal operation residue. With the $+/-$ thresholds defined based on the normal operation class, the value of $rm(t)$ exceeds the negative threshold, triggering the fault flag (Figure 14). It is worth noting that the detection time of the strategy from the moment of fault occurrence to its detection is 0.06 s. This time is given by the difference between the moment the fault flag is activated and the moment the fault occurs. In other words, it is the delay of the system in recognizing a specific fault.
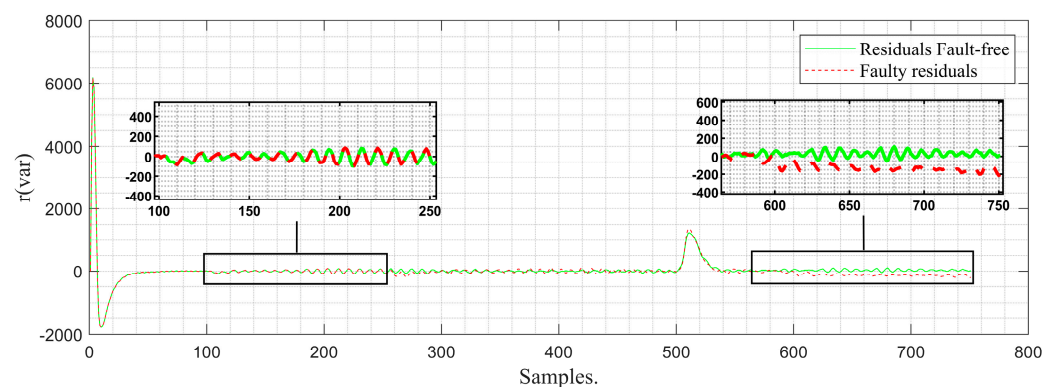

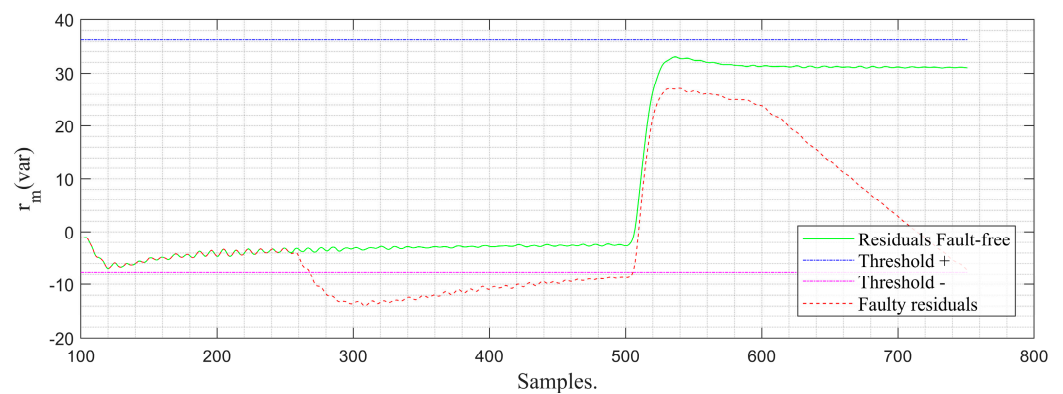**Figure 12.** Residue generation system; incipient fault.

Figure 13. Residue management and fault detection system: mean value of $r(t)$; incipient fault.
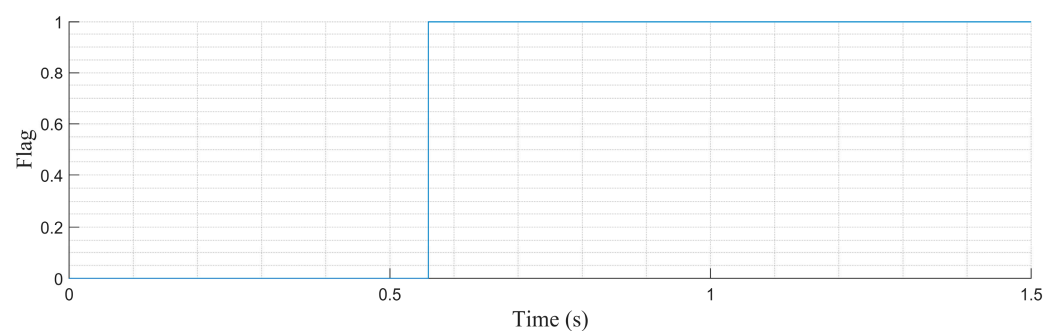

Figure 14. Fault flag; incipient fault.

3.4. Case Study No.4: Random Failure Class

This time, the dynamic behavior of the MG's electrical system in response to a random-type fault is displayed. There is a significant variation over a short period, suggesting that this does not constitute normal sensor behavior. In practice, such variation could be due to various factors, such as a potential loose contact at the connection terminals, issues in the communication channel, or even a cyberattack.

In Figure 15, it is observed that the faulty residues exhibit random behavior with curves that do not follow a defined pattern. This time, the difference between $r(t)$ and $r_m(t)$. is somewhat more noticeable. Figure 16, on the other hand, shows $r_m(t)$ after the residue evaluation procedure of the algorithm. At the time of the fault, the faulty residuals will cross the positive and negative thresholds on various occasions, triggering the fault flag (Figure 17). Once the fault flag is activated, it will remain active until $r_m(t)$ returns within the tolerance band and stays within it for a period of 3 min. This empirical waiting time is selected to ensure that the residual remains within the tolerance band, thus allowing the fault to be cleared. This period guarantees the stabilization of the fault detection system and the correct identification and resolution of any anomaly.
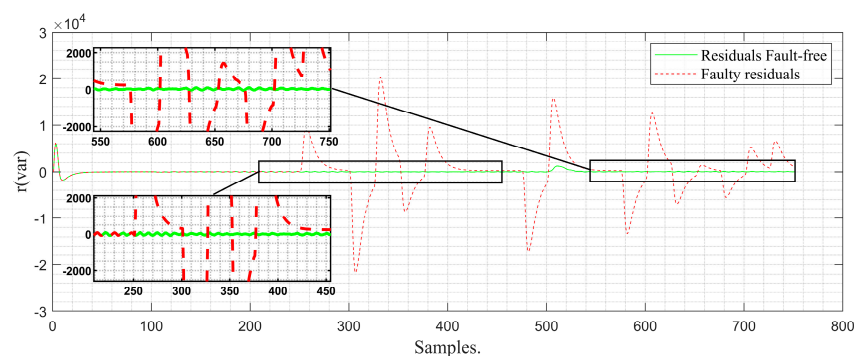

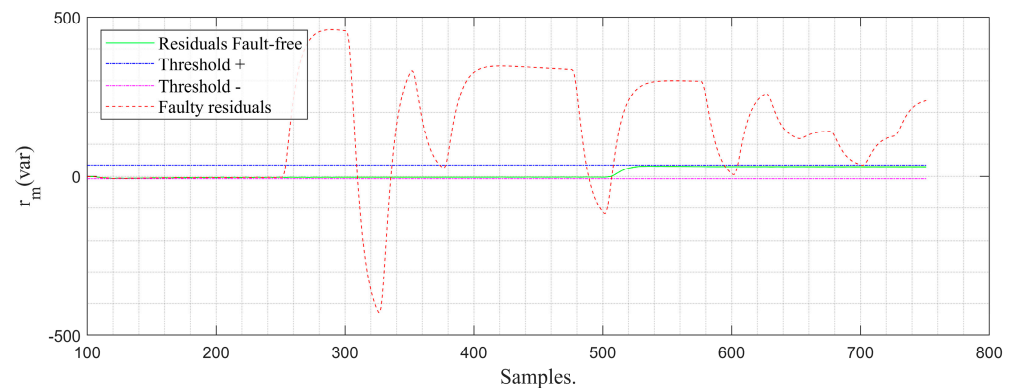**Figure 15.** Residue generation system; random failure.

Figure 16. Residue handling and fault detection system: mean value of $r(t)$; random failure.
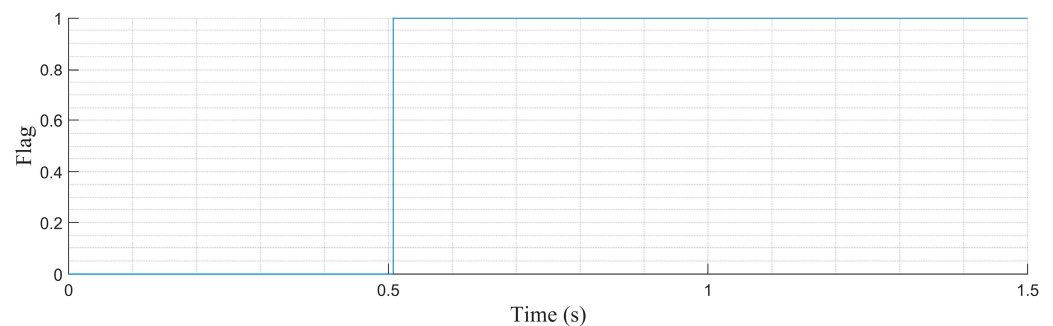

Figure 17. Failure flag; random failure.

4. Results

Table 2 displays the performance metrics of the sensing fault detection strategy, including fault detection time (t_d (s)), observer stabilization time (t_s (s)), and residue value (r_m (var)). The t_d represents the time difference between the fault occurrence and the moment the fault flag is raised at the point where the faulty residue exceeds the thresholds. As shown, this parameter ranges from 0.0075 s to 0.06 s, indicating a rapid system response. On the other hand, the *ts* values range from 0.1 s to 0.88 s and the r_m (in per unit, pu) from 0.0113 pu to 1 pu. These results suggest that the proposed strategy is effective and useful for fault detection systems (FDSs). Figure 18 provides more details, illustrating how the different behaviors defined by the nature of the faults cause the figures to vary.

Table 3 and Figure 19 show the same performance indicators and comparison of the performance that eight authors have managed to obtain in their research when implementing SMO for fault detection has been developed.

Table 2. Proposed sensing Fault Detection System performance.

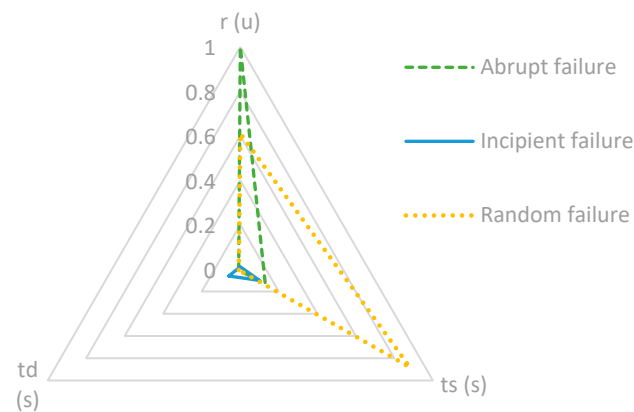| Failure Type	Performance		
	r_m **(var)**	t_s **(s)**	t_d **(s)**
Abrupt failure	1	0.13	0.008
Incipient failure	0.0113	0.1	0.06
Random failure	0.6107	0.88	0.0075

Figure 18. System performance with respect to type of failure.

Table 3. Comparison of the performance of different sensing fault detection methods based on SMO.

Reference	Title/Application	Performance			Observations
		r_m (var)	t_s (s)	t_d (s)	
Current paper.	An On-line Sensor Fault Detection System for AC Microgrid Secondary Control based on a Sliding Mode Observer Model	0.0113 to 1	0.1 to 0.88	0.0075 to 0.06	The application of the method allowed for timely and efficient detection of sensing failures regardless of their type.
[27]	Sensor fault detection and estimation for switched power electronics systems based on sliding mode observer	0.33	0.00076	0.02	The method detects sensing faults, including open circuit faults, with noise anomalies.
[28]	Threshold design for fault detection with first-order sliding mode observers.	-	3	0.01	There is an accurate estimation of failures under idealized assumptions. Constant and time-varying robust thresholds provide guarantees about detection performance.
[29]	A Method based on a Sliding Mode Observer of second order for Fault Detection in Photovoltaic Solar Systems connected to AC Microgrids.	0	0.2	0.04	The method is capable of identifying sensing failures through the residual calculated between the system and the observer.
[30]	Rapid fault reconstruction using a bank of sliding mode observers.	-	1	0.01	The information from the SMOs was used to reconstruct the system and failure states.
[31]	Detection of incipient sensor failures; for application in a high-speed railway traction device with reduced order SMO.	-	-	0.12	The method proposes three levels of new adaptive thresholds based on the dynamics of the reduced-order sliding mode, which effectively improve the detectability of incipient sensor faults.

Table 3. *Cont.*

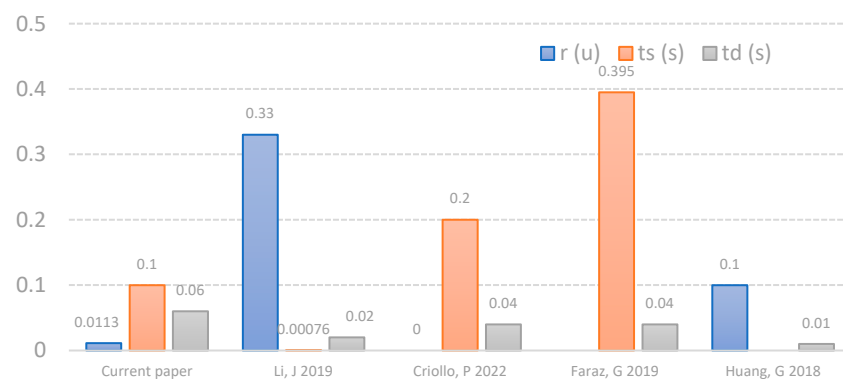| Reference	Title/Application	Performance			Observations
		r_m (var)	t_s (s)	t_d (s)	
[32]	Fault Detection for Mechanical Arm Systems: An Sliding Mode Observer Approach.	-	5	-	The results show that using SMO for fault detection can accurately determine the actual fault, accurately estimate the actual state, and ensure the continuous and trouble-free operation of the system.
[33]	An Integral Sliding Mode Observer Based Fault Diagnosis Approach for Modular Multilevel Converter.	-	0.395	0.04	The method is immune to measurement noise and parameter uncertainties. The scheme can detect and locate faults without being influenced by disturbances.
[34]	Current Sensor Fault Diagnosis Based on Sliding Mode Observer for Permanent Magnet Synchronous Traction Motor.	0–0.1	-	0.01	Simulation and experimental results have demonstrated the feasibility and effectiveness of the method.

Figure 19. Graphic comparison of the performance of principals sensing fault detection methods based on SMO: Li, J 2019 [27], Criollo, P 2022 [29], Faraz, G 2019 [33] and Huang, G 2018 [34].

As previously noted, the Online Sensor Fault Detection System for AC Microgrid Secondary Control based on a Sliding Mode Observer Model offers an effective, simple, and fast solution with low rates of false alarms and robust performance. Thanks to its design, based on SMO, and being programmed through a software application, its practical implementation mainly involves obtaining an accurate model of the system under study, followed by its mathematical design and validation. Afterwards, the algorithm can be downloaded and executed in real-time on an automatic control device.

The implemented fault detection system is based on the model of the sliding mode observer, a robust and efficient technique for monitoring and detecting potential faults in energy systems. This approach is based on the estimation of the system's state by observing its dynamic behavior using a sliding mode observer designed to track discrepancies between the mathematical model of the system and actual measurements. Implementing this system involves integrating control algorithms and data analysis, which enables timely and precise detection of anomalies, thus contributing to the safety and reliability of the energy system.

5. Conclusions

In this research, a fault detection strategy was proposed for a centralized hierarchical control system of a Microgrid using a sliding mode observer. This allows for its implementation in different Microgrid configurations. The results demonstrated an application capable of rapid and timely detection of various faults under study, highlighting its reliability and usefulness in critical operating environments. Moreover, the proposed method can be employed based on a linearized or non-linear system model. This provides a valuable tool for the timely adoption of measures in the reconfiguration of secondary controllers to prevent inappropriate or degraded control actions, which could lead to failures in the physical components of distributed generation sources or storage systems.

The comparative evaluation of eight fault detection system methods proposed by other authors greatly contributed to contextualizing the research in the international field of fault detection in control systems applied to Microgrids. Like the methods consulted in the literature, this research demonstrated remarkable effectiveness in identifying sensed faults, with fault detection times ranging between 0.01 s and 0.12 s. This ensures a real-time and efficient response in emergency situations. In this sense, the application of Robust Observers is positioned as a valuable tool in improving reliability and safety.

Most of the authors consulted achieved significant results in the state estimation of the dynamic systems under study, achieving fault detection times (t_d) between 0.01 s and 0.12 s. However, in some studies, it was observed that the stabilization time was much longer, with values ranging between 0.00076 s and 5 s. These results support the effectiveness of using sliding mode observers for model-based fault detection and their implementation as a tool for fault detection in hierarchical control systems.

The present proposal was validated in a benchmark-type system with Battery Energy Storage Systems, and it focused on two-level centralized hierarchical control, specifically secondary control. Two main structures were proposed: the first is a residue generation system based on robust sliding mode observers, and the second is a residue evaluation system based on the statistical mean. Together, both proposed systems demonstrated excellent performance, simple tuning, and the ability to operate in simulation time.

The practical implementation of such sensing fault detection systems lays the groundwork for future work in fault tolerance, control resilience, and Microgrid isolation. This aims to contribute to the field of Microgrids and fault detection systems, as well as to the reliable, robust, and secure operation of distributed generation systems and storage. This technology also proposes improvements in the quality of the control system input, which is crucial for proper control action functioning.

Finally, future work will aim to complement diagnostic algorithms capable of identifying the root cause of the fault based on its signature, thus preventing cascading failures. Additionally, studies on robustness using other fault conditions (local and tertiary control sensing faults) could be conducted. In this sense, future studies will ensure the system's reliability and its adaptability to different adverse situations. Such systems, along with artificial intelligence, will become assistants and provide real-time corrective measures to improve the detection of other types of faults under real conditions.

Author Contributions: Conceptualization, J.B. and L.O.; Methodology, J.B.; Software, J.B. and L.O.; Validation, J.B., L.O., E.G., M.R. and A.A.; Formal analysis, J.B., L.O., E.G., M.R. and A.A.; Investigation, J.B. and L.O.; Resources, J.B. and L.O.; Writing—original draft, J.B. and L.O.; Writing—review & editing, L.O., E.G., M.R. and A.A.; Visualization, L.O.; Supervision, L.O.; Project administration, L.O. All authors have read and agreed to the published version of the manuscript.

Data Availability Statement: The data presented in this study are available on request from the corresponding author due to privacy.

Conflicts of Interest: The authors declare no conflict of interest.

References

1. Hirsch, A.; Parag, Y.; Guerrero, J. Microgrids: A review of technologies, key drivers, and outstanding issues. *Renew. Sustain. Energy Rev.* **2018**, *90*, 402–411. [CrossRef]
2. Matos, L.O.; Gonzalez Sanchez, J.W. Reconfiguration strategy for Fault Tolerance of power Distribution Systems using Petri net. In Proceedings of the 2016 IEEE Ecuador Technical Chapters Meeting (ETCM), Guayaquil, Ecuador, 12–14 October 2016; IEEE: Guayaquil, Ecuador, 2016; pp. 1–6. [CrossRef]
3. Rogelj, J.; Popp, A.; Calvin, K.V.; Luderer, G.; Emmerling, J.; Gernaat, D.; Fujimori, S.; Strefler, J.; Hasegawa, T.; Marangoni, G.; et al. Scenarios towards limiting global mean temperature increase below 1.5 °C. *Nat. Clim. Change* **2018**, *8*, 325–332. [CrossRef]
4. Al-Ismail, F.S. DC Microgrid Planning, Operation, and Control: A Comprehensive Review. *IEEE Access* **2021**, *9*, 36154–36172. [CrossRef]
5. Papageorgiou, A.; Ashok, A.; Hashemi Farzad, T.; Sundberg, C. Climate change impact of integrating a solar microgrid system into the Swedish electricity grid. *Appl. Energy* **2020**, *268*, 114981. [CrossRef]
6. Angulo, E.; Ruiz, M. *Diseño de Micro Red Eléctrica para Laboratorios de Investigacion Agropecuaria Basado en Optimización Multiobjetivo*; Trabajo de grado- Ingenieria, Universidad Politécnica Salesiana: Quito, Ecuador, 2022. Available online: https://dspace.ups.edu.ec/handle/123456789/23490 (accessed on 1 January 2023).
7. Jirdehi, M.A.; Tabar, V.S.; Ghassemzadeh, S.; Tohidi, S. Different aspects of microgrid management: A comprehensive review. *J. Energy Storage* **2020**, *30*, 101457. [CrossRef]
8. Ortiz-Matos, L.; Zea, L.B.G.; González-Sanchez, J.W. A Methodology of Sensor Fault-Tolerant Control on a Hierarchical Control for Hybrid Microgrids. *IEEE Access* **2023**, *11*, 58078–58098. [CrossRef]
9. Yan, W.; Wang, J.; Lu, S.; Zhou, M.; Peng, X. A Review of Real-Time Fault Diagnosis Methods for Industrial Smart Manufacturing. *Processes* **2023**, *11*, 369. [CrossRef]
10. Zafra-Cabeza, A.; Marquez, J.J.; Bordons, C.; Ridao, M.A. An online stochastic MPC-based fault-tolerant optimization for microgrids. *Control. Eng. Pract.* **2023**, *130*, 105381. [CrossRef]
11. Xie, Z.; Wu, Z. Distributed fault-tolerant secondary control for DC microgrids against false data injection attacks. *Int. J. Electr. Power Energy Syst.* **2023**, *144*, 108599. [CrossRef]
12. Montoya, R.; Poudel, B.P.; Bidram, A.; Reno, M.J. DC microgrid fault detection using multiresolution analysis of traveling waves. *Int. J. Electr. Power Energy Syst.* **2022**, *135*, 107590. [CrossRef]
13. Hu, C.; Wang, M.; Luo, S.; Lu, X.; Huang, Y.; Ma, R.; Fan, H. Fault Diagnosis of DC Microgrid Based on Residual Generator. In Proceedings of the 2021 IEEE 4th International Electrical and Energy Conference (CIEEC), Wuhan, China, 28–30 May 2021; IEEE: Wuhan, China, 2021; pp. 1–6. [CrossRef]
14. Zarei, S.F.; Ghasemi, M.A.; Peyghami, S.; Blaabjerg, F. A Fault Detection Scheme for Islanded-Microgrid with Grid-Forming Inverters. In Proceedings of the 2021 6th IEEE Workshop on the Electronic Grid (eGRID), New Orleans, LA, USA, 8–10 November 2021; IEEE: New Orleans, LA, USA, 2021; pp. 1–6. [CrossRef]
15. Sardashti, A.; Ramezani, A. Fault tolerant control of islanded AC microgrids under sensor and communication link faults using online recursive reduced-order estimation. *Int. J. Electr. Power Energy Syst.* **2021**, *126*, 106578. [CrossRef]
16. Musa, M.H.H.; He, Z.; Fu, L.; Deng, Y. A covariance indices based method for fault detection and classification in a power transmission system during power swing. *Int. J. Electr. Power Energy Syst.* **2019**, *105*, 581–591. [CrossRef]
17. Sardashti, A.; Ramezani, A.; Nezhad, H.S.; Moradmand, A. Observer-based Sensor Fault Detection in Islanded AC Microgrids Using Online Recursive Estimation. In Proceedings of the 2019 6th International Conference on Control, Instrumentation and Automation (ICCIA), Sanandaj, Iran, 30–31 October 2019; IEEE: Sanandaj, Iran, 2019; pp. 1–6. [CrossRef]
18. Sowmmiya, U.; Uma, G. ANFIS-based sensor fault-tolerant control for hybrid grid. *IET Gener. Transm. Distrib.* **2018**, *12*, 31–41. [CrossRef]
19. Li, D.; Yang, H.; Qi, N.; Yuan, J. Observer-based sliding mode control for piezoelectric wing bending-torsion coupling flutter involving delayed output. *J. Vib. Control* **2021**, *27*, 1824–1841. [CrossRef]
20. Mehreganfar, M.; Davari, S.A. Sensorless predictive control method of three-phase AFE rectifier with MRAS observer for robust control. In Proceedings of the 2017 IEEE International Symposium on Predictive Control of Electrical Drives and Power Electronics (PRECEDE), Pilsen, Czech Republic, 4–6 September 2017; IEEE: Pilsen, Czech Republic, 2017; pp. 107–112. [CrossRef]
21. Kavousi-Fard, A.; Su, W.; Jin, T. A Machine-Learning-Based Cyber Attack Detection Model for Wireless Sensor Networks in Microgrids. *IEEE Trans. Ind. Inf.* **2021**, *17*, 650–658. [CrossRef]
22. Mehmood, F.; Khan, B.; Ali, S.M.; Rossiter, J.A. Distributed model predictive based secondary control for economic production and frequency regulation of MG. *IET Control Theory Appl.* **2019**, *13*, 2948–2958. [CrossRef]
23. Ortiz, L.; Orizondo, R.; Águila, A.; González, J.W.; López, G.J.; Isaac, I. Hybrid AC/DC microgrid test system simulation: Grid-connected mode. *Heliyon* **2019**, *5*, e02862. [CrossRef] [PubMed]
24. Wan, Y.; Cao, J.; Chen, G.; Huang, W. Distributed Observer-Based Cyber-Security Control of Complex Dynamical Networks. *IEEE Trans. Circuits Syst. I* **2017**, *64*, 2966–2975. [CrossRef]
25. Amandeep, K.; Jitender, K.; Prasenjit, B. A review on microgrid central controller. *Renew. Sustain. Energy Rev.* **2015**, *55*, 8.
26. Zhang, K.; Jiang, B.; Yan, X.-G.; Mao, Z. Sliding mode observer based incipient sensor fault detection with application to high-speed railway traction device. *ISA Trans.* **2016**, *63*, 49–59. [CrossRef] [PubMed]

27. Li, J.; Pan, K.; Su, Q. Sensor fault detection and estimation for switched power electronics systems based on sliding mode observer. *Appl. Math. Comput.* **2019**, *353*, 282–294. [CrossRef]

28. Keijzer, T.; Ferrari, R.M.G. Threshold design for fault detection with first order sliding mode observers. *Automatica* **2022**, *146*, 110600. [CrossRef]

29. Criollo, P.; Ortiz, L.; Aguila, A.; Pavon, W. A Method based on a Sliding Mode Observer for Fault Detection in Photovoltaic Solar Systems connected to AC Microgrids. In Proceedings of the 2022 IEEE Sixth Ecuador Technical Chapters Meeting (ETCM), Quito, Ecuador, 11–14 October 2022; IEEE: Quito, Ecuador, 2022; pp. 1–6. [CrossRef]

30. Shakarami, M.; Esfandiari, K. Rapid fault reconstruction using a bank of sliding mode observers. *J. Frankl. Inst.* **2022**, *359*, 11229–11255. [CrossRef]

31. Zhang, J.; Swain, A.K.; Nguang, S.K. Robust Estimation of Sensor Faults. In *Robust Observer-Based Fault Diagnosis for Nonlinear Systems Using MATLAB®*; Advances in Industrial Control; Springer International Publishing: Cham, Switzerland, 2016; pp. 87–114. ISBN 978-3-319-32323-7.

32. Jia, T.; Liu, Y.; Li, J. Fault Detection for Mechanical Arm Systems: An Sliding Mode Observer Approach. In Proceedings of the 2019 IEEE 3rd Information Technology, Networking, Electronic and Automation Control Conference (ITNEC), Chengdu, China, 15–17 March 2019; IEEE: Chengdu, China, 2019; pp. 1541–1544. [CrossRef]

33. Faraz, G.; Majid, A.; Khan, B.; Saleem, J.; Rehman, N.U. An Integral Sliding Mode Observer Based Fault Diagnosis Approach for Modular Multilevel Converter. In Proceedings of the 2019 International Conference on Electrical, Communication, and Computer Engineering (ICECCE), Swat, Pakistan, 24–25 July 2019; IEEE: Swat, Pakistan, 2019; pp. 1–6. [CrossRef]

34. Huang, G.; Fukushima, E.F.; She, J.; Zhang, C. Current Sensor Fault Diagnosis Based on Sliding Mode Observer for Permanent Magnet Synchronous Traction Motor. In Proceedings of the 2018 IEEE 27th International Symposium on Industrial Electronics (ISIE), Cairns, QLD, Australia, 12–15 June 2018; IEEE: Cairns, QLD, Australia, 2018; pp. 835–840. [CrossRef]